Simultaneous observations of transient decreases of Earth's far–ultraviolet dayglow with two cameras

L. A. Frank and J. B. Sigwarth
Department of Physics and Astronomy, The University of Iowa, Iowa City

Abstract. The Polar spacecraft carries two cameras which are capable of viewing Earth's far–ultraviolet dayglow. One of these two cameras was programmed into a special operating mode during 12 April and 30 July 1996 in order to obtain simultaneous images of transient decreases of dayglow emissions from atomic oxygen at 130.4 nm. During the 76 minutes of usable imaging the two cameras acquired five sets of frames for which a transient decrease was detected by each camera, and the transient decrease occurred at the same geographical position in the dayglow. These series of observations provide strong evidence for the identification of atmospheric holes as a geophysical phenomenon.

Introduction

Evidence for the existence of transient decreases in Earth's far–ultraviolet dayglow with diameters in the range of 50 to 100 km and their explanation in terms of an influx of small comets has been previously discussed in detail [*Frank and Sigwarth,* 1993]. Our present purpose is to extend the previous observations with simultaneous images of the same atmospheric hole with two cameras on board the recently launched Polar spacecraft.

Observations

The Polar spacecraft was launched into a high–inclination orbit at 86° with apogee over the Northern polar regions. The initial apogee and perigee altitudes of 50,510 km and 5,170 km, respectively, provided splendid viewing of Earth's auroras and dayglow. The orbital period of 17.6 hours offers long viewing periods.

The two cameras for imaging the dayglow at far–ultraviolet wavelengths are mounted on the spacecraft despun platform so that their fields–of–view can continuously stare at Earth, while the main body of the spacecraft which services the in–situ fields–and–particles instruments rotates with a period of 6 s. The two cameras are the Earth Camera of the Visible Imaging System (VIS) [*Frank et al.,* 1995] and the Ultraviolet Imager (UVI) [*Torr et al.,* 1995]. The relevant wavelength for the present investigation is that of the atomic oxygen (OI) emissions at 130.4 nm. The UVI is equipped with a narrow–band filter that isolates this emission from other prominent dayglow emissions. The VIS filter is relatively wide, 124–149 nm. However, the OI 130.4–nm emissions are sufficiently dominant that the VIS images are a record of this emission. The field–of–view of the UVI is approximately circular with a full angle of 8° and that of the VIS is rectangular and 20° × 20°. Thus the solid angle viewed with the VIS is about 8 times larger than that with the UVI. Both the UVI and the VIS imagers are equipped with image intensifiers which feed charge–coupled devices (CCDs). The oval frame of the UVI is dimensioned at 200 × 228 pixels. The square frame of the VIS has 256 × 256 pixels. The corresponding angular dimensions of the pixels are about 0.04° × 0.04° and 0.08° × 0.08° for the UVI and the VIS, respectively. Frame repetition rate for the UVI is typically 39 s but can be reprogrammed with onboard software. The typical frame rates for the VIS are in the range of 12 to 60 s. The present series of measurements are taken at an altitude range of 13,000 to 23,000 km. For reference the dimensions of the UVI and VIS pixels at a range of 15,000 km are about 10.5 and 21 km, respectively. Thus, if the diameter of the atmospheric hole is 50 km then the diameters as detected with the UVI and the VIS are about 5 and 2.5 pixels, respectively. The apparent motions of the atmospheric hole are < 1 and 0.5 pixel/s, respectively.

The spacecraft center–of–gravity could not be positioned along the spin axis with the movable masses within the spacecraft body. As seen looking along the cameras' fields–of–view, there is a cyclic wobble of 0.38° once each spin period of 6 s. The corresponding motions are along one axis of the pixel arrays of the UVI and VIS cameras. The motion of the pixels across the dayglow is substantial, about 100 km, or 10 and 5 pixels for the UVI and VIS images, respectively, at a range of 15,000 km.

Two examples of unprocessed images from the VIS Earth Camera are given in a companion paper, including a description of the rigorous statistical analysis of the pixel responses and the robust identification of atmospheric holes [*Frank and Sigwarth,* 1997a]. A third example of an unprocessed VIS image is given by *Frank and Sigwarth* [1997b]. An example of an unprocessed image from the UVI camera with its 130.4–nm filter is shown in Figure 1. The "mark of Zorro" is seen in the lower left–hand sector of the image, and there is substantial "mottling" and permanent small–scale dark regions in the image. Examination of the series of images revealed the remarkable, infrequent presence of very large clusters of darkened pixels with diameters in the expected range of about 100 km as projected to an altitude of 500 km above Earth's surface. These holes
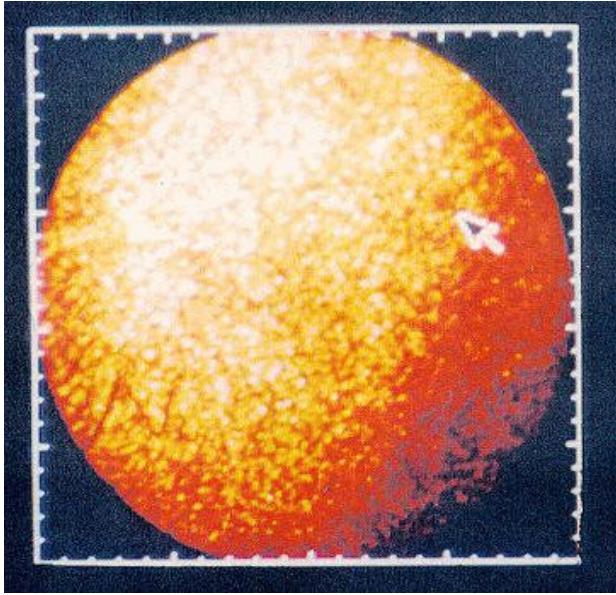
Figure 1. Unprocessed UVI image of Earth's dayglow at 130.4 nm. The frame accumulation time is 22:56:04–22:56:13 on 12 April 1996.

were transient and not seen in the preceding or following images. An example of one of these events is shown at the arrow point in Figure 1. The number of adjacent darkened pixels in this event was impressive, 15 darkened pixels with decreases of −1.5 to −2.8 standard deviations, σ, with the expected substantial fringe of lesser darkened pixels. For the UVI images there were a total of 14 such events easily seen in the raw images. These events were identified as candidate atmospheric holes.

An overview of the two series of images for the identification of atmospheric holes which occurred at the same time and position is given in Table 1. For Period 1 on 12 April 1996 the total observing time was 64 minutes and images from the VIS and the UVI were not electronically despun, i.e., the effects of the 0.38° motion of the platform were not eliminated from the images with on–board software. The sampling times for each frame were reduced to 9 s and 18 s for the UVI and the VIS, respectively, in order to mitigate the effects of this platform motion as noted in the previous section. The number of images and holes detected during Period 1 are also summarized in Table 1. There were two holes detected in near–simultaneous frames with the UVI and the VIS. Because of the requirements that the holes be detected as large clusters of darkened pixels and the fact that the UVI pixel dimension is one half the VIS dimension, the VIS frame must follow in time the UVI frame by 20 to 30 s. This timing takes advantage of the fact that the diameter of the atmospheric hole is increasing at the rate of about 1 km/s [*Frank and Sigwarth,* 1993, 1997a]. The frame time delay must be less than the observed lifetime of atmospheric holes of about 60 to 90 s. The number of such pairs of detections is small due to the infrequency of

Table 1. Special Periods for Simultaneous Atmospheric Hole Observations With the VIS and UVI Cameras

	Period 1	Period 2
Date (1996)	12 April	30 July
Time (UT)	22:54–23:58	05:50–06:02
Number of VIS holes	10	3
Number of UVI images	53	8
Number of UVI holes	11	3
Number of holes in simultaneous frames	2	3
Number of collocated holes in simultaneous frames	2	3

the 9–s UVI frame, one frame every 72 s. The VIS frame was accumulated for 18 s and telemetered every 33 s. For the two sets of near–simultaneous events, the geographical positions as seen with the VIS and the UVI are collocated within the effects of platform wobble, atmospheric hole motion and optical distortions.

An example of the simultaneous detection of the same atmospheric hole with the UVI and VIS imagers is shown in Figures 2 and 3. Figure 2 shows 12 × 12–pixel subframes from the two imagers for the image frames before, during and after the detection of the atmospheric hole. These subframes are all taken at the same locations in their respective images. The frame accumulation times are also given in this figure. The pixel responses are interpolated but the subframes are otherwise unprocessed so that no artifacts arise from image processing. The small scale darkenings are typical of the response fluctuations of single, isolated pixels for the sensors.
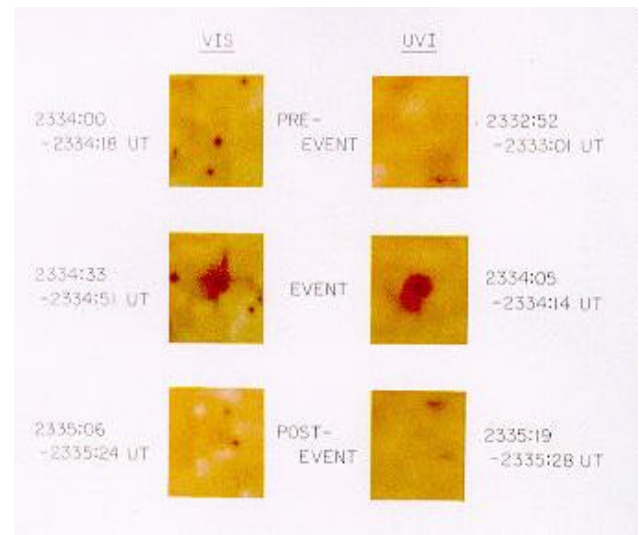
The simultaneous detection of the atmospheric

Figure 2. Subframes of the VIS and UVI images that show the dayglow intensities at the same location in Earth's upper atmosphere before, during and after the occurrence of an atmospheric hole.

POLAR SPACECRAFT
— SIMULTANEOUS DETECTION OF SAME
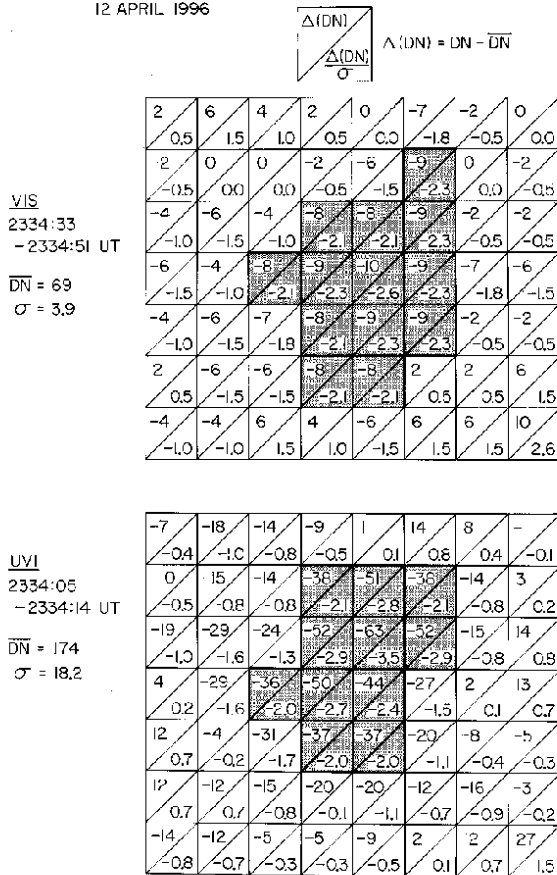ATMOSPHERIC HOLE WITH TWO CAMERAS
12 APRIL 1996

$\Delta(DN)$
$\dfrac{\Delta(DN)}{\sigma}$
$\Delta(DN) = DN - \overline{DN}$

VIS
2334:33
– 2334:51 UT
$\overline{DN} = 69$
$\sigma = 3.9$

UVI
2334:05
– 2334:14 UT
$\overline{DN} = 174$
$\sigma = 18.2$

Figure 3. Pixel maps for the atmospheric hole shown in Figure 2.

hole as shown in Figure 2 is quite impressive in consideration of the infrequency of large hole occurrence in the two sets of images. The pixel maps for the atmospheric hole as observed with the VIS and UVI are shown in Figure 3. The VIS and UVI data are in the raw data formats of the respective cameras. The standard deviations σ and average responses, DN, are given for both sets of pixels. The standard deviations σ and average responses are derived from adjacent pixel blocks in the same image or the same pixel blocks in the preceding or following images, whichever are not compromised by the deposition of charge by penetrating charged particles from the radiation zones. Pixels with $\sigma < -2.1$ (VIS) and -1.9 (UVI) are shaded. The direction of the angular motion of the spacecraft platform is parallel to the horizontal axis. Because of the large fluctuations in UVI responses only clusters with ≥ 10 darkened pixels were identified as atmospheric holes in the present study.

The frame accumulation times, spacecraft geographic coordinates, VIS and UVI hole center location in the (column, row = c, r) format of the VIS

Table 2. Simultaneous Images of Atmospheric Holes With the VIS and UVI Cameras
(VIS and UVI images are not despun)

	A 12 April 1996	B 12 April 1996
VIS frame time (UT)	22:56:40–22:56:58	23:34:33–23:34:51
UVI frame time (UT)	22:56:04–22:56:13	23:34:05–23:34:14
Spacecraft position (geographic, altitude, km)	20.1N, 202,7E, 12,972	42.6N, 195.4E, 19,594
VIS hole (column, row)	(104, 134)	(123, 136)
UVI hole (VIS format, column, row)	(109, 138)	(130,136)
VIS hole position (geographic, range, km)	34.3N, 197.5E, 12,831	46.3N, 190.8E, 19,131
UVI hole position	35.6N, 200.9E, 12,693	48.6N, 197.0E, 19,045

Table 3. Simultaneous Images of Atmospheric Holes With the VIS and UVI Cameras.
(VIS images are despun, UVI images are not despun; Same hole seen in two consecutive VIS images and one UVI image.)

	C 30 July 1996	D 30 July 1996	E 30 July 1996
First VIS frame time (UT)	05:50:20–05:50:56	05:53:01–05:53:37	05:59:17–05:59:53
UVI frame time (UT)	05:50:50–05:50:59	05:53:55–05:54:31	05:59:25–05:59:34
Second VIS frame time (UT)	05:51:14–05:51:50	05:53:55–05:54:31	06:00:10–06:00:46
Spacecraft position (geographic, altitude, km)	26.7N, 351.8E, 16,352	28.3N, 351.3E, 16,817	31.6N, 350.0E, 17,892
First VIS hole (column, row)	(122, 194)	(90, 138)	(105 192)
UVI hole (VIS format, column, row)	(116,200)	(89, 140)	(104, 192)
Second VIS hole (column, row)	(117, 198)	(93, 135)	(101, 185)
First VIS hole position (geographic, range, km)	33.7N, 353.3E, 15,934	24.6N, 0.5E, 16,438	38.6N, 357.7E, 17,523
UVI hole position	34.1N, 354.9E, 16,008	23.4N, 358.0E, 16,461	37.0N, 356.4E, 17,508
Second VIS hole position	35.0N, 355.4E, 16,115	24.6N, 359.8E, 16,586	37.5N, 358.6E, 17,662

EXAMPLE OF "DOUBLE VISION"
    FOR DETECTION OF AN ATMOSPHERIC HOLE
    DUE TO THE ANGULAR MOTION OF THE
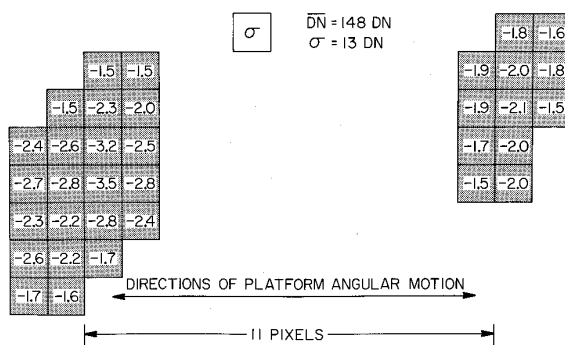   SPACECRAFT PLATFORM

Figure 4. Double vision for detection of an atmospheric hole with the UVI at 2354:56 UT on 12 April 1996 due to angular motion of the unbalanced spacecraft.

images, and the geographic coordinates at 500 km and the range from spacecraft to hole for the VIS and UVI detections during 12 April 1996 are given in Table 2. For a given set of frames the spacecraft position is given for the midpoint of the VIS accumulation interval. Angular motion of the platform is along the abscissa, i.e., across the columns of pixels. The fields−of−view of the two cameras were bore−sighted at 1400 UT on 31 May 1996 while viewing the star HD 120315. Examination of the contents of this table finds excellent agreement of the positions of the atmospheric holes as determined with the two imagers to within the accuracy allowed by the motions of the spacecraft platform and the atmospheric hole.

For Period 2 on 30 July 1996 the observing time was 12 minutes. For this series of observations the VIS images were electronically despun which greatly increased this instrument's capability for detecting atmospheric holes. In addition the percentage of the time for sampling the VIS images increased because the frame time is 36 s with a repetition time of 54 s. During Period 2 three atmospheric holes were detected in the UVI images and also three in the VIS images (see Table 1). All three holes were collocated in the images from the two imagers. In fact the VIS is able to detect the same atmospheric hole in two consecutive images. The first hole in each set is necessarily weaker [*Frank and Sigwarth,* 1997a]. The atmospheric hole is detected in a single UVI frame.

It is further reassuring that the UVI images of atmospheric holes sometimes exhibit the effects of the angular motion of the platform with period 6 s and amplitude of 0.38°. This produces a "double vision" of an object in the camera's field−of−view due to the projection of this circular motion, i.e., two ansae have an increased sampling time and thus two darkened clusters

are present for a single object. The amplitude of the angular motion corresponds to about 11 UVI pixels. An example is shown in Figure 4. The spacecraft is viewing Earth from an altitude of 22,800 km at geographic coordinates 50.5° N and 191.5° E. Because the frame accumulation time is 9.2 s and the spin period is 6 s the two ansae will be unequally sampled. The ansa on the left has been accumulated for twice as long as the right−hand ansa. The darkening is correspondingly about twice as dark for the left−hand ansa, as expected. Such a constrained observation eliminates instrumental artifacts.

This double−vision effect was often masked by the brightenings due to penetrating charged particles in the CCD sensor. Only four of the 11 UVI holes detected on 12 April exhibited the cat's eyes or the sawteeth (for events with faster angular motion) because the dimmer eyes or teeth were washed out by the penetrating charged particles. For most of the present observations the Polar spacecraft is located at high altitudes on magnetic L−shells in the range of L) 3 to 5, i.e., in the large fluxes of penetrating electrons in the radiation zones. The range of > 5−MeV electron fluxes is ~5×10^3 to 5×10^4/cm^2−s [*McIlwain,* 1963]. For an estimated 10% efficiency for producing ionization in a pixel and a 9−s frame integration time the number of pixels with such ionization events will range from 5,000 to 50,000 pixels. The pixel map of Figure 4 was obtained at positions outside of the radiation zones and thus the weaker "eye" on the right−hand side was preserved. This weaker eye is not preserved in Figure 1 when the Polar spacecraft was deeply within the radiation zones at L) 3.4. This double vision, or "cat's eyes", has been reported also for the VIS camera [*Frank and Sigwarth,* 1997a].

During the analyses of the images from the UVI it became apparent that the UVI was generally not capable of identifying a darkened cluster as due to a real object or electronic noise without confirmation from an independent camera. This is due to its insufficient time resolution to detect the holes in consecutive images and to eliminate the effects of platform motion. On the other hand, the images with the VIS Earth Camera were characterized by the elimination of the smearing due to platform motion and by a frame repetition rate sufficient to detect the atmospheric holes in two consecutive images [*Frank and Sigwarth,* 1997a]. To the point, the VIS Earth Camera was capable of independently verifying that the darkened clusters of pixels were not instrument artifacts.

A measure of the statistical significance of the successful simultaneous detections is provided by using a bucket of 40 pixels, thus with 220 buckets per image. For only one event (or ball) every 3 images one is left in the situation of randomly throwing this ball at $220 \times 3 = 660$ buckets in the hope of hitting the correct bucket with no misses. The presently reported simultaneous detections are clearly robust.

Summary

The purpose of this paper is the presentation of simultaneous observations of the same transient decreases of Earth's far−ultraviolet dayglow intensities, or atmospheric holes, with two independent cameras on board the Polar spacecraft. These simultaneous observations of atmospheric holes with the two Polar cameras as reported here provide confirmation that they are a geophysical phenomenon.

References

Frank, L. A. and J. B. Sigwarth, "Atmospheric holes and small comets", *Rev. Geophys*., 31, 1−28, 1993.

Frank, L. A., et al., "The visible imaging system (VIS) for the Polar spacecraft", *Space Sci. Rev., 71,* 297−328, 1995.

Frank, L. A. and J. B. Sigwarth, "Transient decreases of Earth's far−ultraviolet dayglow", *Geophys. Res. Lett.,* (this issue), 1997a.

Frank, L. A. and J. B. Sigwarth, "Detection of atomic oxygen trails of small comets in the vicinity of Earth", *Geophys. Res. Lett.,* (this issue), 1997b.

McIlwain, C. E., "The radiation belts, natural and artificial", *Science, 142,* 355−361, 1963.

Torr, M. R., et al., "A far ultraviolet imager for the International Solar−Terrestrial Physics Mission", *Space Sci. Rev., 71,* 329−383, 1995.

L. A. Frank and J. B. Sigwarth, Department of Physics and Astronomy, The University of Iowa, Van Allen Hall, Iowa City, IA 52242.
(e−mail: frank@iowasp.physics.uiowa.edu;
sigwarth@iowasp.physics.uiowa.edu)